Substructuring and poroelastic modelling of the intervertebral disc

Pascal Swider, Annaïg Pedrono, Dominique Ambard, Franck Accadbled, Jérôme Sales de Gauzy

Substructuring and poroelastic modelling of the intervertebral disc

P. Swider [a,*], A . Pédrono [a], D. Ambard [b], F. Accadbled [c], J. Sales de Gauzy [c]

[a] IMFT UMR CNRS 5502, University of Toulouse, CHU Purpan, Amphithéâtre Laporte, Place Dr Baylac, 31056 Toulouse cedex, France
[b] LMGC UMR CNRS 5508, University of Montpellier, France
[c] Department of Pediatric Orthopedics, Children Hospital, Toulouse, France

We proposed a substructure technique to predict the time-dependant response of biological tissue within the framework of a finite element resolution. Theoretical considerations in poroelasticity preceded the calculation of the sub-structured poroelastic matrix. The transient response was obtained using an exponential fitting method. We computed the creep response of an MRI 3D reconstructed L_5–S_1 intervertebral disc of a scoliotic spine. The FE model was reduced from 10,000 degrees of freedom for the full 3D disc to only 40 degrees of freedom for the sub-structured model defined by 10 nodes attached to junction nodes located on both lower and upper surfaces of the disc. Comparisons of displacement fields were made between the full poroelastic FE model and the sub-structured model in three different loading conditions: compression, offset compression and torsion. Discrepancies in displacement were lower than 10% for the first time steps when time-dependant events were significant. The substructuring technique provided an exact solution in quasi-static behavior after pressure relaxation. Couplings between vertical and transversal displacements predicted by the reference FE model were well stored by the sub-structured model despite the drastic reduction of degrees of freedom. Finally, we demonstrated that substructuring was very efficient to reduce the size of numerical models while respecting the time-dependant behavior of the structure. This result highlighted the potential interest of substructure techniques in large-scale models of musculoskeletal structures.

1. Introduction

Numerous computational models have been developed to investigate the biomechanical behavior of the spine (Stokes and Laible, 1990; Lavaste et al., 1992). Complex models involved non-linearities such as vertebrae fractures, contacts between articular facets, and non-linear behaviors of ligaments and muscles (Smit, 1996; Dolan and Adams, 2001; Imai et al., 2006; Noailly et al., 2007). Advanced models of intervertebral discs have also been implemented (Simon et al., 1985; Argoubi and Shirazi-Adl, 1996; Frijns et al., 1997; Martinez et al., 1997; Lee et al., 2000). The relevance of predictive models increased along with their complexity. However, it appears that management of non-linear behavior is computationally time consuming and it is still difficult to cumulate the description of local effects in predictive large-scale models. This difficulty has been particularly limitative to intervertebral disc modelling whereas disc local behavior and global behavior of the spine interact in the pathogenesis of spine (Périé et al., 2003; Brisby, 2006; Natarajan et al., 2006).

The substructuring technique associated with the finite element method proved to be of great interest in computational mechanics in linear statics and dynamics. The robustness of the method has been shown and its limitations have been discussed (Lalanne et al., 1983; Zienkiewicz et al., 2005). This method was used to predict the mechanical behavior of a complex structure by dividing the structure into a series of smaller structures, called substructures, and studying the intrinsic behavior of these components. Substructuring allowed a considerable reduction in the number of degrees of freedom, which would otherwise be required to model the entire initial structure. In linear behavior, the underlying assumption of this technique was that the superposition principle of elasticity was applicable. This technique has been adapted to cases where non-linear behavior was confined to certain parts of the structures, such stress concentrations, crack tips, non-linear material and mounts (Hellen, 1984; Gjika et al., 1996).

In our study, we hypothesized that the substructuring technique could be relevant in case of non-linear elastic structure with poroelastic behavior. The substructuring technique was applied to an intervertebral disc within sight, the potential use in larger computational model of vertebral segments. The creep response of a L_5–S_1 intervertebral disc reconstructed from MRI was investigated.

* Corresponding author. Tel.: +33 5 61 49 79 44; fax: +33 5 61 49 67 45.
E-mail address: swider@cict.fr (P. Swider).

Nomenclature

u^s	displacement of structural phase
u^f	displacement of fluid phase
u^{fs}	displacement of fluid vs structural phase
$\dot{u}, \ddot{u}$	velocity, acceleration
ϕ	tissue porosity
p	interstitial fluid pressure
σ_{ij}	stress tensor
ρ, ρ^s, ρ^f	densities
q^f	flow rate of the fluid phase
μ^f	fluid dynamic viscosity
k^s	compressibility of structural phase
k^f	compressibility of fluid phase
k^f	compressibility modulus of fluid
α	Biot coefficient
κ_{ij}	specific permeability tensor
ε, ξ	volume strain, permeability decay factor
K	structural stiffness matrix
M	mass matrix
Q	fluid-structure matrix
H	permeability matrix
C_t	tangent stiffness matrix,
B	strain–displacement matrix
N^u, N^p	shape functions
P	poroelastic matrix
f^u, f^p	structural and flux nodal forces
δ, δ^e, δ^i	dof, external dof, internal dof
$\overline{P}$	sub-structured poroelastic matrix
f	equivalent nodal force
f^u, f^p	nodal force vector, nodal fluid flux
u^e, p^e	external nodal displacement and pressure
u^i, p^i	internal nodal displacement and pressure
$\overline{u}^e$	displacements of sub-structured model
f^e, f^i	external and internal nodal forces
f^{ue}, f^{ui}	external and internal nodal forces
f^{pe}, f^{pi}	external and internal nodal flux
η	decay factor
$e_{\%}$	error criterion in displacement

2. Material and methods

2.1. Poroelastic governing equations

The continuum was modeled using two phases: the structural phase Ω^s and the fluid phase Ω^f. The conservation of momentum of fluid phase neglecting fluid velocity gradient led to the generalized Darcy Law (1) (Biot, 1941; Coussy, 1995; Meroi et al., 1999). The conservation of momentum for structural phase was expressed by Eq. (2), and the continuity equation of fluid phase was given by Eq. (3).

$$q_i^f = \phi \dot{u}_i^{fs} = \frac{\kappa_{ij}}{\mu_f}\left[-p_{,j} + \rho^f (g_j - \ddot{u}_j^s - \ddot{u}_j^{fs})\right] \tag{1}$$

$$\sigma_{ji,j} + \rho g_i = \rho \ddot{u}_i^s + \phi \rho^f (\ddot{u}_i^{fs} + \dot{u}_i^{fs} \dot{u}_{i,i}^{fs}) \tag{2}$$

$$\dot{u}_{i,i}^s + \left[\frac{(\alpha-\phi)}{k^s} + \frac{\phi}{k^f}\right]\dot{p} + q_{i,i}^f + q_i^f \frac{\rho_{,i}^f}{\rho^f} = 0 \tag{3}$$

Boundary conditions (4) were imposed displacements d and imposed force σ on $(\Gamma^d, \Gamma^\sigma)$ of the structural phase Ω^s. Imposed flux and imposed pressure on (Γ^q, Γ^p) concerned the fluid phase Ω^f.

$$u^s(x,t) = d \text{ for } x \in \Gamma^d \ \sigma(x,t)n = \sigma \text{ for } x \in \Gamma^\sigma \tag{4}$$

$$p(x,t) = p \text{ for } x \in \Gamma^p \ q_i^i n = q \text{ for } x \in \Gamma^q$$

Within the finite element resolution, the previous continuous problem was formulated using the matrix system (5) where nodal degrees of freedom (dof) were the displacement field u and the pressure field p (Pédrono, 2001). Related elementary matrices and vectors are briefly listed in Appendix.

$$\frac{1}{2}Ku^s - Qp - M\ddot{u}^s = f^u \text{ and } Hp + Q^t \dot{u}^s = f^p \tag{5}$$

Additional assumptions were made in the theoretical model. The structural phase Ω^s was isotropic, incompressible and involved small strains ($k^s = +\infty$, $\alpha = 1$). The fluid phase Ω^f was incompressible ($k^f = +\infty, \rho_i^f = 0$). Filtration terms ($\ddot{u}_i^{fs}, \dot{u}_i^{fs}\dot{u}_{i,i}^{fs}$) and accelerations in the Darcy law were neglected (Coussy, 1995).

2.2. Adaptation of the substructuring technique

The resolution of system (5) was achieved using a linearization scheme in time and space. This was obtained using a time Newmark finite difference scheme of order 2 for displacement and order 1 for pressure. The Newton–Raphson algorithm (Kelley, 2003) was added for local linearization and convergence. Finally, the non-linear problem (5) was transformed into system (6) at each time step and P was called the poroelastic matrix.

$$P\delta = f \text{ with } P = \begin{bmatrix} p_1 & p_3 \\ p_4 & p_2 \end{bmatrix} \tag{6}$$

And ${}^t d = ({}^t d^e; {}^t d^i) = (u^e, p^e; u^i, p^i)$ ${}^t f = ({}^t f^e; {}^t f^i) = (f^{u_e}, f^{p_e}; f^{u_i}, f^{p_i})$

Matrix system (6) was expressed separating internal dof δ^i and external dof δ^e. The external dof δ^e were associated to nodes of the initial FE Meshing representing a junction between the zone of interest or sub-structured domain and the complementary structures. The internal dof δ^i concerned nodes of the complementary meshing of the disc involving nucleus puplosus and annulus fibrosus.

The management of internal dof δ^i as matrix functions of external dof δ^e was the basis of the substructuring procedure. Matrix P involved four sub-matrices: p_1, p_2, p_3 and p_4. The quasi-static equilibrium was computed at each time step which allowed establishing the linear dependence of internal dof δ^i with selected external dof δ^e. Internal dof δ^i were replaced by external dof δ^e using the second line of system (6). The result was put into the first line of (6) to obtain the sub-structured poroelastic matrix $\overline{P}$ expressed by Eq. (7). The size of (7) was dependant upon the number of external dof δ^e.

$$\overline{P}\delta^e = \overline{f} \text{ with } \overline{P} = (p_1 - p_3 p_2^{-1} p_4) \tag{7}$$

and

$${}^t\delta^e = (u^e, p^e) \quad \delta^i = -p_2^{-1} p_4 \delta^e + p_2^{-1} f^i \quad \overline{f} = f^e - p_3 p_2^{-1} f^i$$

When the creep response was investigated, the time-dependant computation of system (6) at time $t=0$ allowed computation of each term of the initial sub-structured matrix $\overline{P}_0$. This matrix combined contributions of structural matrix K, fluid matrix H and fluid-structure coupling matrix Q. At time $t=+\infty$, influence of fluid pressure was negligible due to pressure relaxation and the viscoelastic response converged towards the quasi-static linear response. As a result, sub-structured poroelastic matrix $\overline{P}_\infty$ was obtained by suppressing the contribution of pressure dof in system (7). Between these two states, $t=0$ and $t=+\infty$, the time-dependant poroelastic matrix $\overline{P}(t)$ was fitted using an exponential form with a decay factor η as expressed by Eq. (8).

$$\overline{P}(t) = \overline{P}_{+\infty} + (\overline{P}_0 - \overline{P}_{+\infty}) e^{-\eta t} \tag{8}$$

Finally, the computational model was implemented in Python programming language (Python Software Foundation®) using Pysparse module to solve the spatio-temporal finite element matrix systems. Only one full computation of the initial matrix system (5) and the decay factor η were required to predict the time response of the substructure, which was beneficial in terms of computation time saving.

2.3. Application to a L_5–S_1 intervertebral disc

MRI images of the L_5–S_1 segment of a twelve-year-old male scoliotic patient were obtained using a turbo spin echo T_2-weighted MRI sequence (Magneton Vision, 1.5 T). This was achieved according to a validated clinical infant method (Violas et al., 2005). The global coordinate system was defined according to JCS (*Joint Coordinate System)* (Wu et al., 2002). Cranial part and caudal part of the disc included the outer layers of vertebral end plates. As shown in Fig. 1, contour segmentation, volume reconstruction and meshing were achieved using a custom-made image processing software developed with Python®.

Marc/Mentat (MSC software®), a finite element-based commercial code, was used to calculate the transient behavior of the intervertebral disc. The meshing was constituted by mixed brick-20 Hermann elements with 3 dof in displacement and 1 dof in pressure per node. The model involved 462 elements, 250 nodes and

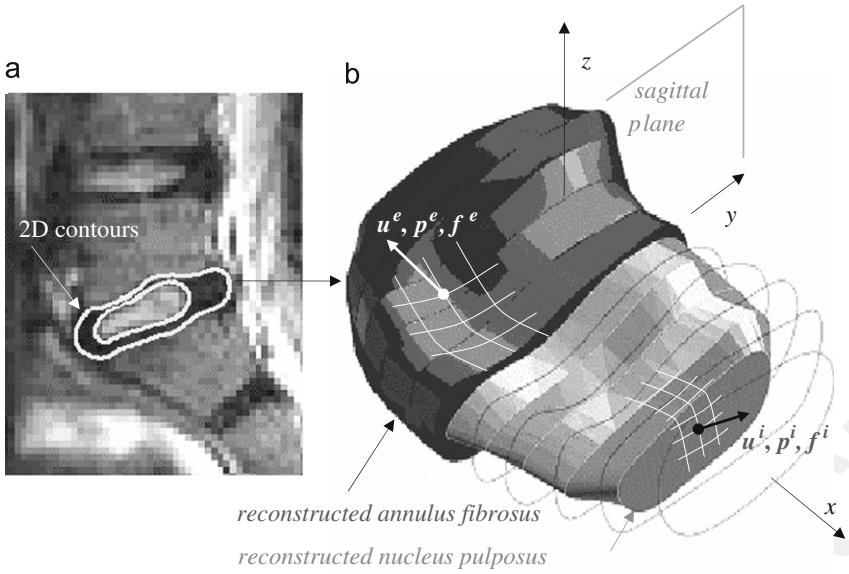

Fig. 1. Application of the substructuring to a L_5–S_1 intervertebral disc. The 3D geometry was reconstructed from MRI: (a) T2-weighted image in the sagittal plane and segmentation of contours, and (b) volume reconstruction of nucleus pulposus and annulus fibrosus. The FE meshing was separated between the internal degree of freedomt ${}^t\delta^i=(u^i,p^i)$ and the external degree of freedom ${}^t\delta^e=(u^e,p^e)$ associated to junction nodes. Internal nodal force f^i was also separated from external nodal force f^e.

10,000 dof. Material properties of a disc were linear isotropic. Young modulus E was 3 MPa for the annulus fibrosus and vertebral end-plate and 1.5 MPa for the nucleus pulposus, Poisson ratio ν was 0.1 for each structure (Argoubi and Shirazi-Adl, 1996; Martinez et al., 1997). Permeability κ/μ was identical for the annulus fibrosus and the nucleus pulposus and it was strain dependant with an initial porosity of $\phi=0.7$ as described in Appendix (A2). Fluid boundary conditions were permeation through the vertebral end plates and sealing on the outer annulus wall. The creep response was predicted under three types of loadings: compression (Fig. 2a), offset compression (Fig. 2b) and torsion (Fig. 2c). Loadings were punctual loads of magnitude 100 N applied during 6000 s. We assumed that displacements fields derived from this full FE model were reliable to be used as a reference to validate the method that we proposed.

In the substructuring, the external dof δ^e nodes were associated with 10 nodes (2×5 nodes) located on the upper and lower surfaces of the disc as shown in Fig. 2. These nodes were selected to represent the junction with vertebral bodies. The size of matrix $\overline{P}(t)$ was 40×40. It corresponded to a matrix formed by 10 nodes with four dof per node: three displacements u^e and one pressure p^e as previously detailed in Eq. (7). We compared time responses of the sub-structured model governed by Eq. (8) with the response of the full model governed by system (5) used as a reference. Error between the two sets of results was given by criterion (9) with u_i^e, $\overline{u}_i^e$, i, respectively being reference displacements, displacements of the sub-structured model and the time step.

$$e_{\%}=\sum_i(\overline{u}_i^e-u_i^e)^2/\sum_i u_i^{e2} \tag{9}$$

3. Results

Time responses of the disc were plotted in Fig. 2d–f for both full poroelastic model and substructured model.With the sub-structuring technique, size reduction of the model was important since a division by 250 was obtained. In addition, computation time was divided by 10^3. The initial computation time of about 20 min was reduced to a few seconds with the sub-structured model.

We focused on response of nodes 1 and 2, located in the centre and in the periphery, respectively. Comparison of displacements showed that maximum discrepancies appeared in the initial time-steps when non-linear effects were significant. Maximum value of criterion $e_{\%}$ was 10% and it was obtained in compression for the central zone of the disc (node 1). Time response was perfectly predicted with the sub-structured model after pressure relaxation ($t=+\infty$) whatever the zone of interest and the loading type.

Results also showed that coupling effects were very well predicted despite the drastic reduction of model size. This clearly appeared in offset compression as shown in Fig. 2e. Compression in z-direction induced a significant transverse translation u in x-direction. In addition, torsion loading induced displacements u and v in the x–y plane but also out-of-plane displacement w in z-direction as shown in Fig. 2f.

In Eq. (8), the time fitting technique of poroelastic matrix $\overline{P}(t)$was managed using the decay factor η. In first approximation, we assumed that this factor was constant in time. Its magnitude was empirically updated by minimizing criterion $e_{\%}$ applied to displacements of nodes 1 and 2. After successive trials, the procedure converged towards a mean value of 0.05 that provided good results for the three types of loadings.

4. Discussion and conclusion

We proposed an adaptation of the substructuring technique to predict the non-linear time response of biological tissue. The formulation was adapted to the creep response using the governing equations of poroelasticity associated with a resolution by the finite element method. Our strategy resulted in describing the mechanical behavior of the biological structure by using a condensed poroelastic matrix and a decay factor.

The underlying principle of the substructuring technique was that a limited number of degrees of freedom would be relevant enough to provide a good approximation of the mechanical energies involved in the complete structure. In the poroelastic formulation, governing energies were associated to structural matrix K, fluid matrix H and fluid-structure matrix Q, with univocal dependence of pore pressure with displacement. Under the same mechanical loadings, a reliable sub-structured model should provide a good approximation of displacements fields compared to those of the complete FE model. The concept of finite element interpolation into a remeshed domain and strain/stress calculations was unrelated the substructuring technique. Only substitution of initial degree of freedom and condensation of associated matrices were required and the study of displacement

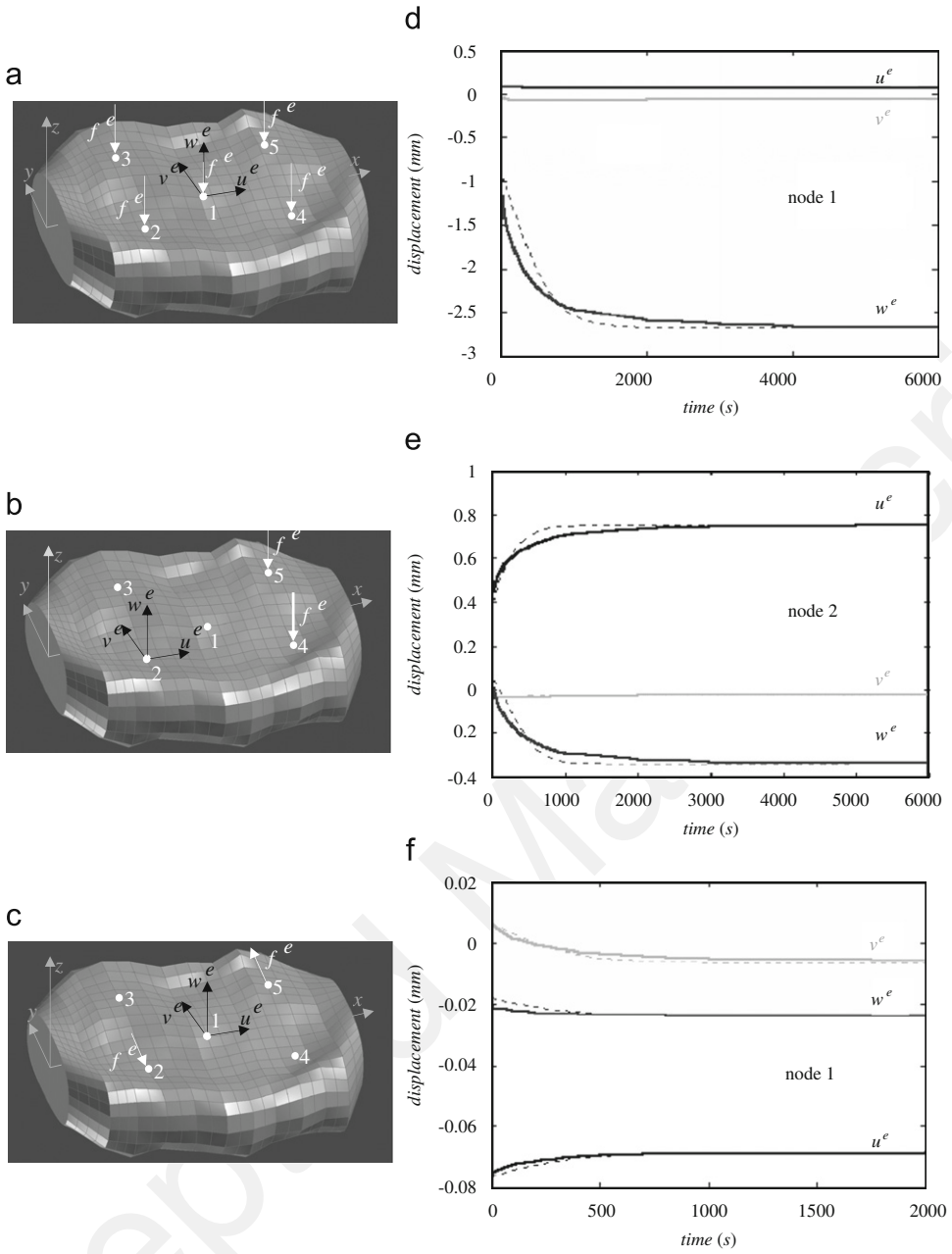

Fig. 2. Validation of the substructure technique: application to a L_5–S_1 intervertebral disc. The creep response was predicted with three types of loadings: (a) and (d) compression, (b) and (e) offset compression, (c) and (f) torsion. External nodes (or junction nodes 1–5) were located on the upper and lower surfaces of the disc in order to establish junctions with vertebral bodies. Transient responses of nodes 1 and 2 were compared: – full FE model (10^3 dof);– sub-structured model (40 dof).

fields was the basis to investigate the accuracy of the substructure procedure.

When the creep response of a L_5–S_1 intervertebral disc was investigated, the whole disc was considered as the actual sub-structure. The external degrees of freedom were attached to nodes selected to provide the junction with vertebral bodies for a potential integration into a larger model i.e. a vertebral segment or the whole spine.

The disc geometry was obtained from MRI in a clinical setting. Hydration levels were used for segmentation of contours but no information about tissue mechanical properties was available. Data from the literature were used to run the full FE model that provided displacement fields in agreement with published results (Argoubi and Shirazi-Adl, 1996; Jones and Wilcox, 2008; Malandrino et al., 2009). This was the base of the validation of the substructuring technique applied to the disc.

The sub-structured model showed very good prediction after fluid pressure relaxation whatever the loading type. This was in agreement with results obtained in general engineering structures (Lalanne et al., 1983; Zienkiewicz et al., 2005) operating in linear behavior. This result highlighted the potential interest of substructuring technique for large-scale FE models of musculoskeletal structures. Transient responses were also well predicted despite drastic reduction of the number of degrees of freedom. The condensed poroelastic matrix was balanced by a decreasing exponential function with a constant decay factor at first approximation. This choice was in agreement with the underlying principle of substructuring which placed at the forefront the reduction of numerical model and computation costs savings.

We found that subtle behavior noticed in published works such as warping and coupling effects (Gardner-Morse and Stokes, 2004; Costi et al., 2007; Violas, 2006) were predicted by the

reference FE model and well stored by the sub-structured model despite the drastic reduction of degrees of freedom. These effects were coupled motion between vertical and transversal displacement fields due to disc geometry and distribution pattern of material properties such as the offset of the nucleus pulposus. This was of interest knowing that these mechanical couplings play a role in the mechanobiology of the disc and in the homeostasis of the vertebral segment.

Variations in patient-specific properties could modify discrepancies between the full and the sub-structured models. The model could be improved while implementing anisotropic or non-linear properties relative to elastic coefficients and permeability of the constitutive tissue. Even if this goal seems attractive, progress in process robustness must be measured and tissue properties investigated in-vivo.

Shifts in tissue elastic coefficient would have no effect on the elastic response since the principle of superposition is warranted by the technique. In return, associated with permeability variations, they could influence the fluid-structure couplings which effects on displacement fields could not be superimposed. The global update using the decay factor η is a relevant way to overcome this difficulty, keeping in mind the compromise between accuracy and model reduction. In this context, signal-processing techniques (Le Fichoux et al., 1999) associated with the substructuring could be of interest to identify tissue properties in-vivo and to predict response to complex transient loading.

Conflict of interest statement

The authors hereby declare to have no conflict of interest.

References

Argoubi, M., Shirazi-Adl, A., 1996. Poroelastic creep response analysis of a lumbar motion segment in compression. J. Biomech. 29 (10), 1331–1339.

Biot, M.A., 1941. General theory of three-dimensional consolidation. J. Appl. Phys. 12, 155–164.

Brisby, H., 2006. Pathology and possible mechanisms of nervous system response to disc degeneration. J. Bone Joint Surg. Am. 88 (suppl 2), 68–71.

Costi, J.J., Stokes, I.A., Gardner-Morse, M., Laible, J.P., Scoffone, H.M., Iatridis, J.C., 2007. Direct measurement of intervertebral disc maximum shear strain in six degrees of freedom: motions that place disc tissue at risk of injury. J. Biomech. 40 (11), 2457–2466.

Coussy, O., 1995. Mechanics of Porous Continua. John Wiley & Sons.

Dolan, P., Adams, M.A., 2001. Recent advances in lumbar spinal mechanics and their significance for modelling. Clin. Biomech. 16 (supplement 1), S8–S16.

Frijns, A.J.H., Huyghe, J.M., Janssen, J.D., 1997. A validation of the quadratic mixture theory for intervertebral disc tissue. Int. J. Eng. Sci. 35, 1419–1429.

Gardner-Morse, M.G., Stokes, I.A., 2004. Structural behavior of human lumbar spinal motion segments. J. Biomech. 37 (2), 205–212.

Gjika, K., Dufour, R., Ferraris, G., 1996. Transient response of structures on viscoelastic or elastoplastic mounts: prediction and experiment. J. Sound Vib. 198 3 (5), 361–378.

Hellen, T.K., 1984. Use of substructuring in non-linear material analysis. Eng. Comput. 1 (4), 343–350.

Imai, K., Ohnishi, I., Bessho, M., Nakamura, K., 2006. Nonlinear finite element model predicts vertebral bone strength and fracture site. Spine 31 (16), 1789–1794.

Jones, A.C., Wilcox, R.K., 2008. Finite element analysis of the spine: towards a framework of verification, validation and sensitivity analysis. Med. Eng. Phys. 30 (10), 1287–1304.

Kelley, C.T., 2003. Solving Nonlinear Equations with Newton's Method, no 1 in Fundamentals of Algorithms. SIAM.

Lalanne, M., Berthier, P., Der Hagopian, J., 1983. Mech. Vib. Eng.. Wiley Interscience, Europe.

Lavaste, F., Skalli, W., Robin, S., Roy-Camille, R., Mazel, C., 1992. Three-dimensional geometrical and mechanical modelling of the lumbar spine. J. Biomech. 25 (10), 1153–1164.

Lee, C.K., Kim, Y.E., Lee, C.S., Hong, Y.M., Jung, J.M., Goel, V.K., 2000. Impact response of the intervertebral disc in a finite-element model. Spine 25 (19), 2431–2439.

Le Fichoux, B., Swider, P., Mouzin, O., 1999. Identification of non-linear transient behaviour of flexible structures; application to a golfer's swing. Mech. Sys. Sig. Proc. J. 13 (3), 509–522.

Malandrino A., Planell J.A., Lacroix D. 2009. Statistical factorial analysis on the poroelastic material properties sensitivity of the lumbar intervertebral disc under compression, flexion and axial rotation. J. Biomech. Epub. Ahead of Print.

Martinez, J.B., Oloyede, V.O.A., Broom, N.D., 1997. Biomechanics of load-bearing of the intervertebral disc: an experimental and finite element model. Med. Eng. Phys. 19 (2), 145–156.

Natarajan, R.N., Williams, J.R., Andersson, G.B., 2006. Modeling changes in intervertebral disc mechanics with degeneration. J. Bone Joint Surg. Am. 88 (suppl 2), 36–40.

Noailly, J., Wilke, H.J., Planell, J.A., Lacroix, D., 2007. How does the geometry affect the internal biomechanics of a lumbar spine bi-segment finite element model ? Consequences on the validation process. J. Biomech. 40 (11), 2414–2425.

Meroi, E.A., Natali, A.N., Schrefler, B.A., 1999. A poroelastic approach to the analysis of the spinal motion segment. Comp. Meth. Biomech. Biomed. Eng. 2 (3), 157–170.

Pédrono, A., 2001. Prévision du comportement poroélastique d'un segment vertébral ; formulation par éléments finis mixtes, MSc Dissertation. University of Toulouse, France.

Périé, D., Curnier, D., de Gauzy, J.S., 2003. Correlation between nucleus zone migration within scoliotic intervertebral discs and mechnaical properties distribution within scoliotic vertebrae. Magn. Reson. Imaging 21 (9), 949–953.

Simon, B.R., Wu, J.S.S., Carlton, M.W., Evans, J.H., Kazarian, L.E., 1985. Structural models for human spinal motion segments based on a poroelastic view of the intervertebral disk. J. Biomech. Eng. 107, 327–335.

Smit, T.H., 1996. The mechanical significance of the trabecular bone architecture in a human vertebra. Ph.D. Thesis. TU Hamburg–Harburg. Shaker Verlag, Aachen, Germany.

Stokes, I.A., Laible, J.P., 1990. Three-dimensional osseo-ligamentous model of the thorax representing initiation of scoliosis by asymmetric growth. J. Biomech. 23 (6), 589–595.

Violas, P., 2006. Contribution à l'étude des disques intervertéraux sous-jacents à une arthrodèse vertébrale postérieure dans la scoliose idiopathique; modélisation à partir de l'IRM, Ph.D. Dissertation. University of Toulouse, France.

Violas, P., Estivalèzes, E., Pédrono, A., Sales de Gauzy, J., Sévely, A., Swider, P., 2005. A method to investigate intervertebral disc morphology from MRI in early idiopathic scoliosis: a preliminary evaluation in a group of 14 patients. Magn. Reson. Imaging 23 (3), 475–479.

Wu, G., Siegler, S., Allard, P., Kirtley, C., Leardini, A., Rosenbaum, D., Whittle, M., D'Lima, D.D., Cristofolini, L., Witte, H., Schmid, O., Stokes, I., 2002. ISB recommendation on definitions of joint coordinate system of various joints for the reporting of human joint motion–part I: ankle, hip, spine. J. Biomech. 35, 543–548.

Zienkiewicz, O.C., Taylor, R.L., Zhu, J.Z., 2005. The Finite Element Method, its Basis & Fundamental. 6th edition Butterworth Heinemann.

Appendix

Resolution of non-linear matrix system (5)

System (5) was solved using a time Newmark finite difference scheme, order 2 for displacement and order 1 for pressure. Initial non-linear system (A1) became linear using the Newton-Raphson method. F^u and F^p were force components and θ, β_1 and β_2 were parameters of time integration scheme. Stiffness matrix K and fluid-structure matrix Q were updated at each time step. Mass matrix M was independent from strain.

$$\begin{bmatrix} \frac{1}{2}K\beta_1\Delta t^2 - M & -Q\theta\Delta t \\ -Q^t\theta\Delta t & -\frac{\theta^2}{\beta_2}H\Delta t \end{bmatrix} \begin{pmatrix} \Delta\ddot{u} \\ \Delta\dot{p} \end{pmatrix} = \begin{Bmatrix} F^u \\ -\frac{\theta}{\beta_2}F^p \end{Bmatrix} \tag{A1}$$

with $K = \int_v {}^t B\ C_t\ B\ dv$ $M = \int_v {}^t N^u\ \rho\ N^u\ dv$ $Q = \int_v {}^t B\ m\ N^p dv$ $m = (1,1,1,0,0,0)^t$

$$H = \int_v {}^t(\nabla N^p)\ \frac{\kappa_{ij}}{\mu}\ \nabla N^p\ dv \qquad f^u = \int_{\Gamma^\sigma} {}^t N^u f\ d\Gamma^\sigma \qquad f^p = -\int_{\Gamma^p} N_p{}^t q\ d\Gamma^p$$

Permeability of annulus fibrosus and nucleus pulposus was strain-dependant according to the governing equation (A2) (Martinez et al. 1997).

$$\frac{\kappa}{\mu}(\varepsilon) = (\kappa/\mu)_{+\infty} + \left[(\kappa/\mu)_0 - (\kappa/\mu)_{+\infty}\right] e^{(\varepsilon/\xi)} \tag{A2}$$

with $(\kappa/\mu)_0 = 1.10^{-15}$ m^4/Ns $(\kappa/\mu)_{+\infty} = 7.10^{-16}$ m^4/Ns $\xi = 0.1$